



**HAL**  
open science

# Systematics of Nd cumulative fission yields for neutron-induced fission of $^{235}\text{U}$ , $^{238}\text{U}$ , $^{238}\text{Pu}$ , $^{239}\text{Pu}$ , $^{240}\text{Pu}$ and $^{241}\text{Pu}$

G. Noguere, J. Tommasi, E. Privas, K.-H. Schmidt, D. Rochman

► **To cite this version:**

G. Noguere, J. Tommasi, E. Privas, K.-H. Schmidt, D. Rochman. Systematics of Nd cumulative fission yields for neutron-induced fission of  $^{235}\text{U}$ ,  $^{238}\text{U}$ ,  $^{238}\text{Pu}$ ,  $^{239}\text{Pu}$ ,  $^{240}\text{Pu}$  and  $^{241}\text{Pu}$ . The European Physical Journal Plus, 2018, 133, 99, 10.1140/epjp/i2018-11926-y . cea-02339854

**HAL Id: cea-02339854**

**<https://hal-cea.archives-ouvertes.fr/cea-02339854>**

Submitted on 5 Nov 2019

**HAL** is a multi-disciplinary open access archive for the deposit and dissemination of scientific research documents, whether they are published or not. The documents may come from teaching and research institutions in France or abroad, or from public or private research centers.

L'archive ouverte pluridisciplinaire **HAL**, est destinée au dépôt et à la diffusion de documents scientifiques de niveau recherche, publiés ou non, émanant des établissements d'enseignement et de recherche français ou étrangers, des laboratoires publics ou privés.

# Systematics of Nd cumulative fission yields for neutron-induced fission of $^{235}\text{U}$ , $^{238}\text{U}$ , $^{238}\text{Pu}$ , $^{239}\text{Pu}$ , $^{240}\text{Pu}$ and $^{241}\text{Pu}$ .

G. Noguere, J. Tommasi, E. Privas,

*CEA, DEN Cadarache, 13108 Saint Paul Les Durance, France*

K.-H. Schmidt

*Centre d'Etudes Nucléaires Bordeaux Gradignan,*

*CNRS/IN2P3, Univ. Bordeaux 1, 33175 Gradignan, France*

D. Rochman

*Paul Scherrer Institut, 5232 Villigen, Switzerland*

(Dated: January 9, 2018)

## Abstract

Systematics of cumulative fission yields of the Neodymium isotopes for thermal and fast neutron fission of  $^{235}\text{U}$ ,  $^{238}\text{U}$ ,  $^{238}\text{Pu}$ ,  $^{239}\text{Pu}$ ,  $^{240}\text{Pu}$  and  $^{241}\text{Pu}$  were obtained by combining integral results from the PROFIL experiments with theoretical calculations from the GEF code. The systematic behavior with the Neodymium mass number ( $A = 143, 145, 146, 148, 150$ ) deduced from the experimental trends is consistent with the smooth variation predicted by the GEF calculations, excepted for the  $^{238}\text{U}(n,f)$  reaction. For this system, isotopic and isotonic effects in fission-fragment shell structures are not adequately taken into account in the theoretical calculation. The obtained results also confirm the weak energy dependence of the Nd cumulative fission yields in the energy range of interest for thermal and sodium fast reactors. They suggest an energy dependency comparable to the experimental uncertainty which lies below 3%, for the  $^{235}\text{U}$ ,  $^{239}\text{Pu}$  and  $^{241}\text{Pu}$  fissile isotopes.

## I. INTRODUCTION

The irradiation experiments PROFIL-1, PROFIL-2A and PROFIL-2B were carried out in the fast reactor PHENIX (CEA Marcoule, France). Their interpretations with the deterministic code ERANOS [1] have provided a large amount of integral trends [2–4]. Some of them are sensitive to the cumulative fission yields of  $^{143}\text{Nd}$ ,  $^{145}\text{Nd}$ ,  $^{146}\text{Nd}$ ,  $^{148}\text{Nd}$  and  $^{150}\text{Nd}$ . The Neodymium isotopes of interest for this work are all stable nuclides. In that case, the corresponding cumulative fission yield represents the total number of atoms of that nuclide remaining per fission after the decay of all precursors. Figure 1 illustrates the 148-decay chain to  $^{148}\text{Nd}$ . The Nd isotopes have several neutronic advantages compared with other fission products. They are known to be characterized by a linear behavior with respect to burnup of nuclear fuel. Among the neodymium isotopes,  $^{148}\text{Nd}$  is identified as an ideal burn-up monitor for determining the time-integrated neutron flux and scaling the reactor power history.

Effective cumulative fission yields obtained for the  $^{235}\text{U}(\text{n},\text{f})$  reaction were already reported in Ref. [6] with a preliminary investigation of the performances of the semi-empirical model implemented in the GEF code [7]. As a result, GEF seems to be a suitable tool to handle the variation of the cumulative fission yields with the incident neutron energy.

The present work aims to complement the previous analysis by reporting Nd cumulative fission yields not only for  $^{235}\text{U}(\text{n},\text{f})$  but also for  $^{238}\text{U}$ ,  $^{238}\text{Pu}$ ,  $^{239}\text{Pu}$ ,  $^{240}\text{Pu}$  and  $^{241}\text{Pu}$  from thermal (25.3 meV) to fast energy ranges ( $\simeq 400$  keV). The same methodology, as used for  $^{235}\text{U}$ , was applied to extract experimental fission yields averaged over the fast neutron spectrum of the PHENIX reactor. The typical relative uncertainty that can be reached is lower than 3%, for  $^{235}\text{U}$ ,  $^{239}\text{Pu}$  and  $^{241}\text{Pu}$ .

For determining values at the thermal energy, we decided to normalize the cumulative fission yields calculated with the GEF code by using the PROFIL trends. The reliability of such a simplified approach was verified with a standard Integral Data Assimilation (IDA) procedure [8]. Due to the smooth and weak variation with the energy, strong correlations exist between the thermal and fast energy ranges. These correlations allowed to estimate the thermal cumulative fission yields of the Nd isotopes with relative uncertainties ranging from 2% to 5%, even for  $^{238}\text{U}$ ,  $^{238}\text{Pu}$  and  $^{240}\text{Pu}$  whose cumulative fission yields are poorly known.

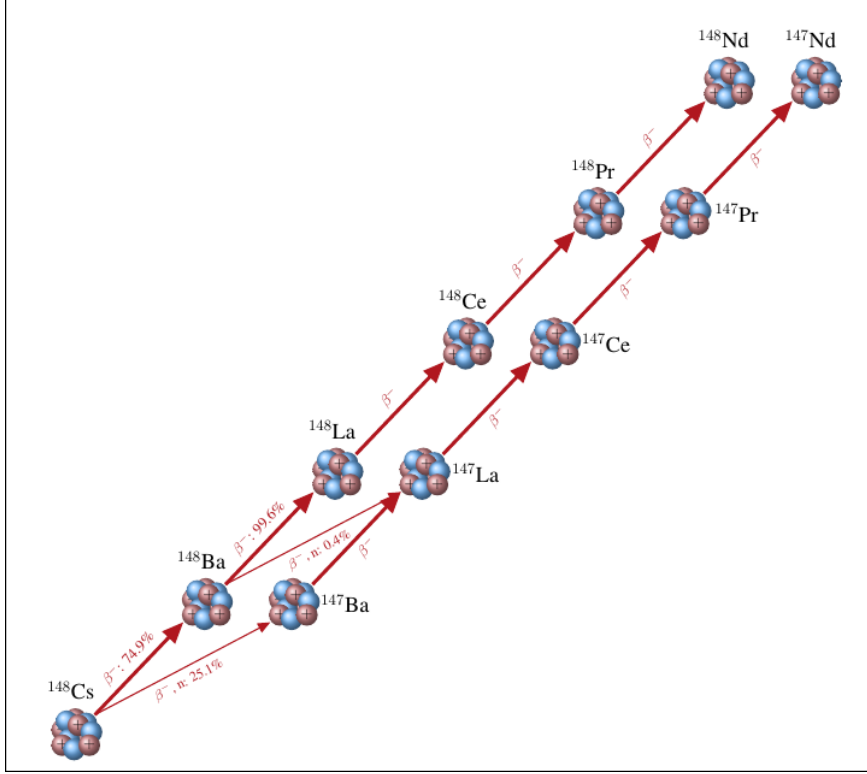


FIG. 1: Example of decay scheme for isotopes with mass equal to 148 taken from Ref [5].

The consistency of our results expressed as a function of the mass number ( $A = 143, 145, 146, 148, 150$ ) and of the neutron energy are discussed throughout the paper by looking the behavior of the evaluated values compiled in the international libraries JEFF-3.1.1 [9] and ENDF/B-VII.1 [10]. The overall good agreement achieved for the most important fissile targets ( $^{235}\text{U}$ ,  $^{239}\text{Pu}$  and  $^{241}\text{Pu}$ ) suggests that the combined analysis of the PROFIL results with the GEF calculations offers a set of valuable data for improving the theoretical parametrization around the Nd isotopes over a wide neutron energy range.

## II. GOVERNING EQUATIONS

Since the methodology used in this work has been already applied on  $^{235}\text{U}$ , only the most important features of the PROFIL experiments and of the theoretical background are briefly given in the present document. More detailed explanations can be found in Ref. [6].

The principle of the PROFIL experiments consisted of irradiating samples containing a small amount of pure isotope in the fast neutron flux of the PHENIX reactor (CEA Mar-

coule, France). Experimental results ( $E$ ) are the isotopic composition of the samples before and after the irradiation period. The theoretical results ( $C$ ) were calculated with the ERANOS code in association with the nuclear data library JEFF-3.1.1. In the present work, we are interested in the calculated-to-experimental ratios  $\langle C/E \rangle_X$  related to the Neodymium content produced in the studied samples after fission of a given actinide  $X$ . Since the ERANOS calculations were performed by using the fast cumulative fission yields  $Y_{c_j}^X(^A\text{Nd}, E_n)$  of the JEFF-3.1.1 library given at  $E_n=400$  keV, effective cumulative fission yield  $\bar{Y}_{cp}^X(^A\text{Nd})$  can be determined from the PROFIL results as follows:

$$\bar{Y}_{cp}^X(^A\text{Nd}) = Y_{c_j}^X(^A\text{Nd}, E_n = 400 \text{ keV}) + \Delta\bar{Y}_{cp}^X(^A\text{Nd}), \quad (1)$$

where  $\Delta\bar{Y}_{cp}^X(^A\text{Nd})$  is related to the calculated-to-experimental ratios  $\langle C/E \rangle_X$  via the sensitivity coefficient  $S(^A\text{Nd})$  of  $C$  to the cumulative fission yields of the Neodymium isotope  $^A\text{Nd}$ :

$$\frac{\Delta\langle C/E \rangle_X}{\langle C/E \rangle_X} = S(^A\text{Nd}) \frac{\Delta\bar{Y}_{cp}^X(^A\text{Nd})}{Y_{c_j}^X(^A\text{Nd}, E_n)}, \quad (2)$$

with the condition:

$$\langle C/E \rangle_X + \Delta\langle C/E \rangle_X = 1. \quad (3)$$

By introducing Eqs (2) and (3) in Eq (1), we obtain:

$$\bar{Y}_{cp}^X(^A\text{Nd}) = \left( 1 + \frac{1 - \langle C/E \rangle_X}{S(^A\text{Nd})\langle C/E \rangle_X} \right) Y_{c_j}^X(^A\text{Nd}, E_n = 400 \text{ keV}), \quad (4)$$

The GEF code, in association with the Q-matrix formalism [11], is able to provide cumulative fission yields  $Y_{c_g}^X(^A\text{Nd}, E)$  as a function of the incident neutron energy  $E_n$ . The model implemented in GEF is empirical. Several parameters are adjusted to reproduce experimental data. However, it relies on physical notions, which permits to limit the amount of parameters, and to use the same set of parameters for all fissioning systems over a large excitation energy range. Results obtained for the  $^{235}\text{U}(n,f)$  reaction are shown in Fig. 2. For the comparison with the PROFIL values, GEF results have to be averaged over the fission reaction rate:

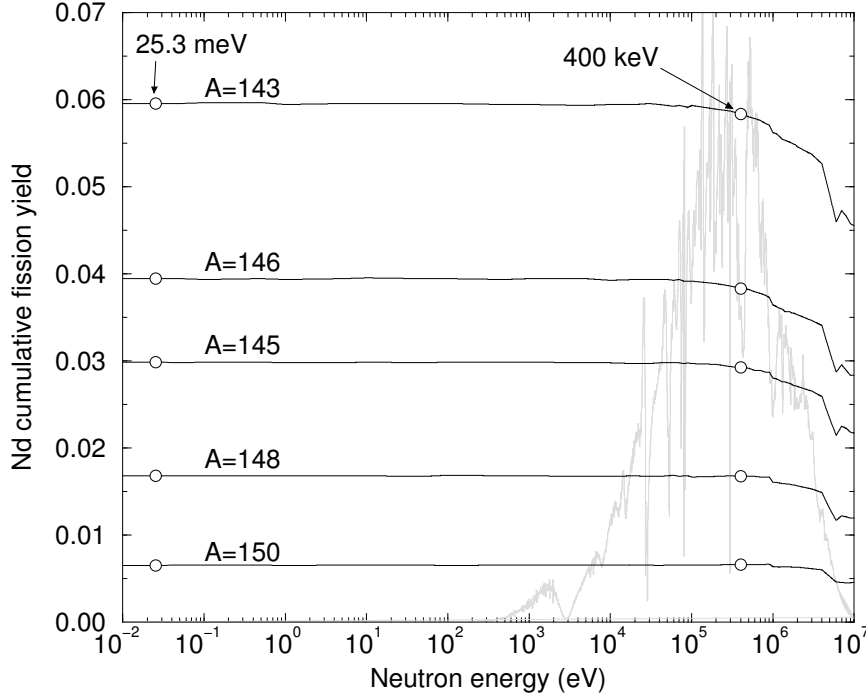


FIG. 2: The black lines are the Nd cumulative fission yields as a function of the incident neutron energy for  $^{235}\text{U}$  calculated with the GEF code [7]. They are compared to a neutron spectrum (grey line), in arbitrary units, representative of the PROFIL experiments [2–4]. The open circles indicate the position of the thermal energy (25.3 meV) and fast neutron energy (400 keV).

$$\bar{Y}_{cG}^X(A\text{Nd}) = N \frac{\int_0^{E_{max}} Y_{cG}^X(A\text{Nd}, E_n) \sigma_{fX}(E_n) \phi(E_n) dE_n}{\int_0^{E_{max}} \sigma_{fX}(E_n) \phi(E_n) dE_n}, \quad (5)$$

in which  $\phi(E_n)$  stands for the fast neutron spectrum representative of the PROFIL experiment. It is shown in Fig. 2 as a function of the incident neutron energy  $E_n$ . The fission cross sections  $\sigma_{fX}(E_n)$  of interest for this work are shown in Fig 3. The maximum energy  $E_{max}$  is set to 20 MeV. The normalization factor  $N$  is equal to unity.

Assessment of cumulative fission yields at the thermal energy from PROFIL results consists in determining the energy dependent cumulative fission yields  $Y_{cG}^X(A\text{Nd}, E_n)$  in order to satisfy the following relationship:

$$\bar{Y}_{cG}^X(A\text{Nd}) = \bar{Y}_{cP}^X(A\text{Nd}). \quad (6)$$

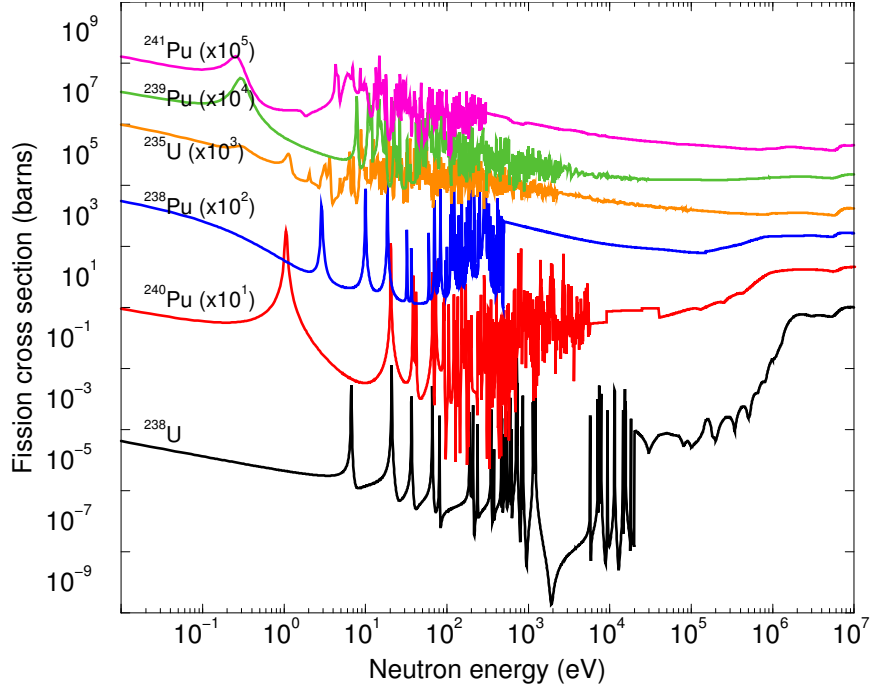


FIG. 3: Fission cross sections of  $^{235}\text{U}$ ,  $^{238}\text{U}$ ,  $^{238}\text{Pu}$ ,  $^{239}\text{Pu}$ ,  $^{240}\text{Pu}$  and  $^{241}\text{Pu}$  recommended in the Joint Evaluated Fission and Fusion library JEFF-3.1.1 [9].

The problem can be solved either by using standard Integral Data Assimilation procedures, for which reliable prior covariances between the fission yields are needed, or by scaling the GEF results via the normalization factor  $N$ . Results obtained by the two methods are discussed in section IV.

### III. CUMULATIVE FISSION YIELDS IN THE FAST ENERGY RANGE

#### A. Average calculated-to-experimental ratios from PROFIL

Crucial ingredients in Eq. (4) are the calculated-to-experimental ratios  $\langle C/E \rangle_X$  calculated for a given actinide  $X$ . However, after the irradiation period, the quantity of Neodymium measured by Inductively Coupled Plasma Mass Spectrometry results from the fission of all actinides present in the studied sample. As a result, calculated-to-experimental ratios  $\langle C/E \rangle$  account for all these contributions, noted  $X$  in the following expression:

$$\langle C/E \rangle \simeq \sum_X \omega_X(\bar{\phi}) (\langle C/E \rangle_X + \delta_f(X)), \quad (7)$$

with the condition:

$$\sum_X \omega_X(\bar{\phi}) = 1. \quad (8)$$

The weight  $\omega_X$  associated to each fissile isotope  $X$  depends on the fluence level  $\bar{\phi}$ . The correction term  $\delta_f(X)$  is introduced to account for possible biases on the calculations of the Neodymium content due to the theoretical fission cross sections used in the ERANOS calculations.

We have used ERANOS results to estimate the values of  $\omega_X$  as a function of the fluence. In the  $^{238}\text{U}$  samples, the Neodymium isotopes are mainly produced via the  $^{238}\text{U}(\text{n,f})$ ,  $^{239}\text{Pu}(\text{n,f})$  and  $^{235}\text{U}(\text{n,f})$  reactions with weights equal to 0.659, 0.326 and 0.015, respectively, for an average fluence of  $\bar{\phi} = 10.0 \times 10^{22} \text{ n/cm}^2$ . In the  $^{238}\text{Pu}$  sample, the main contributions come from the  $^{238}\text{Pu}(\text{n,f})$  and  $^{239}\text{Pu}(\text{n,f})$  reactions. The weights are close to 0.85 and 0.15, respectively, for  $\bar{\phi} = 9.2 \times 10^{22} \text{ n/cm}^2$ . In the  $^{240}\text{Pu}$  sample, the weights associated to the  $^{240}\text{Pu}(\text{n,f})$ ,  $^{241}\text{Pu}(\text{n,f})$ ,  $^{238}\text{Pu}(\text{n,f})$  and  $^{239}\text{Pu}(\text{n,f})$  reactions are 0.805, 0.177, 0.012 and 0.006 ( $\bar{\phi} = 17.3 \times 10^{22} \text{ n/cm}^2$ ). For the  $^{235}\text{U}$ ,  $^{239}\text{Pu}$  and  $^{241}\text{Pu}$  samples, contributions from other fission reactions are negligible and the weights  $\omega_X$  are assumed to be close to unity. The uncertainty on each  $\omega_X$  is set to  $\pm 0.01$ .

In Eq. (7), the order of magnitude of the correction term  $\delta_f(X)$  depends on the evaluated fission cross sections tabulated in the JEFF-3.1.1 library (Fig. 3). It can be estimated with fission indices measured in fast critical mock-up reactors. Weighted averages of few calculated-to-experimental ratios measured in the MASURCA [12], PROTEUS [13, 14] and FCA [16] facilities have led to the following correction terms for the  $^{238}\text{U}(\text{n,f})$ ,  $^{238}\text{Pu}(\text{n,f})$ ,  $^{239}\text{Pu}(\text{n,f})$ ,  $^{240}\text{Pu}(\text{n,f})$  and  $^{241}\text{Pu}(\text{n,f})$  reactions:

$$\delta_f(^{238}\text{U}) = -0.009 \pm 0.009,$$

$$\delta_f(^{238}\text{Pu}) = +0.140 \pm 0.020,$$

$$\delta_f(^{239}\text{Pu}) = -0.018 \pm 0.007,$$

$$\delta_f(^{240}\text{Pu}) = +0.030 \pm 0.014,$$



$$\delta_f(^{241}\text{Pu}) = -0.004 \pm 0.021.$$

All corrections terms lie below  $\pm 3\%$ , excepted the one related to  $^{238}\text{Pu}$ . According to the obtained result, the  $^{238}\text{Pu}$  fission cross section of JEFF-3.1.1 is overestimated by 14%. Consequently, cumulative fission yields determined from the  $^{238}\text{Pu}$  samples should be considered with care. No correction is applied to the  $^{235}\text{U}$  fission cross section because it was used to scale the fluence level.

Table I reports the calculated-to-experimental ratios  $\langle C/E \rangle$  of the Neodymium buildup averaged over the individual  $C/E$  ratios obtained from the PROFIL-1, PROFIL-2A and PROFIL-2B experiments. They were calculated with the ERANOS code by using the evaluated nuclear data of the JEFF-3.1.1 library. The quoted uncertainties are only the statistical uncertainties coming from the Inductively Coupled Plasma Mass Spectrometry. The corrected ratios  $\langle C/E \rangle_X$  are given in Table II. The reported uncertainties include the uncertainties of the weights  $\omega_X$  and correction terms  $\delta_f(X)$ . They remain below  $\pm 3.5\%$  for all the calculated-to-experimental ratios. Such rather low relative uncertainties will ensure an accurate estimation of the effective cumulative fission yields in the fast energy range.

## B. Effective cumulative fission yields

Effective cumulative fission yields of  $^{143}\text{Nd}$ ,  $^{145}\text{Nd}$ ,  $^{146}\text{Nd}$ ,  $^{148}\text{Nd}$  and  $^{150}\text{Nd}$  have been deduced from the calculated-to-experimental ratios  $\langle C/E \rangle_X$  listed in Table II by using Eq. (4). Results are given in Table III. The quoted uncertainties take into account the accuracy of  $S(^A\text{Nd})$ , which is the sensitivity coefficient of  $C$  to the cumulative fission yields of the Neodymium isotope  $^A\text{Nd}$ , and the uncertainty due to the fluence scaling procedure. The value of  $S(^A\text{Nd})$  is close to unity and the associated relative uncertainty is set to 2%. The fluence scaling procedure has been carefully studied in Ref. [4]. Since the well-known fission cross section of  $^{235}\text{U}$  was taken as reference for the interpretation of the PROFIL experiments, the relative uncertainty is rather low ( $< 2\%$ ).

In the same Table, our results are compared with fast cumulative fission yields evaluated in the international library JEFF-3.1.1 and in the US library ENDF/B-VII.1. The differences between all the values depend on the fissile isotope and on the library. However, we can note that the agreement between most of the values extracted from the PROFIL results and those from the JEFF-3.1.1 and ENDF/B-VII.1 libraries remains within the limit of the

TABLE I: Average calculated-to-experimental ratios  $\langle C/E \rangle$  of the Neodymium buildup for the PROFIL-1, PROFIL-2A and PROFIL-2B experiments. The numbers in the brackets indicate the number of experimental values used in the average. The quoted uncertainties take only into account the isotopic ratio uncertainties provided by Inductively Coupled Plasma Mass Spectrometry.

Sample	$^{143}\text{Nd}$	$^{145}\text{Nd}$	$^{146}\text{Nd}$	$^{148}\text{Nd}$	$^{150}\text{Nd}$
$^{235}\text{U}$ (9)	$0.985\pm 0.003$	$1.022\pm 0.003$	$1.032\pm 0.003$	$1.034\pm 0.002$	$1.057\pm 0.003$
$^{238}\text{U}$ (3)	$0.963\pm 0.008$	$0.964\pm 0.008$	$0.981\pm 0.008$	$1.012\pm 0.009$	$0.968\pm 0.008$
$^{238}\text{Pu}$ (1)	$1.193\pm 0.012$	$1.324\pm 0.013$	$1.361\pm 0.014$	$1.322\pm 0.013$	$1.185\pm 0.012$
$^{239}\text{Pu}$ (2)	$0.965\pm 0.003$	$0.993\pm 0.005$	$1.011\pm 0.003$	$1.011\pm 0.002$	$1.003\pm 0.003$
$^{240}\text{Pu}$ (1)	-	-	-	$1.023\pm 0.020$	-
$^{241}\text{Pu}$ (2)	$0.989\pm 0.007$	$0.990\pm 0.007$	$1.003\pm 0.007$	$1.008\pm 0.007$	$0.991\pm 0.007$

TABLE II: Calculated-to-experimental ratios  $\langle C/E \rangle_X$  determined from values reported in Table I after subtraction of the fission contributions from other actinides and corrected by the term  $\delta_f(X)$  (Eq. (7)). The quoted uncertainties account for the isotopic ratio uncertainties provided by Inductively Coupled Plasma Mass Spectrometry, the uncertainties of the correction terms  $\delta_f(X)$  and of the weights  $\omega_X$ .

Sample	$^{143}\text{Nd}$	$^{145}\text{Nd}$	$^{146}\text{Nd}$	$^{148}\text{Nd}$	$^{150}\text{Nd}$
$^{235}\text{U}$	$0.985\pm 0.003$	$1.022\pm 0.003$	$1.032\pm 0.003$	$1.034\pm 0.002$	$1.057\pm 0.003$
$^{238}\text{U}$	$0.971\pm 0.028$	$0.958\pm 0.028$	$0.974\pm 0.029$	$1.021\pm 0.029$	$0.957\pm 0.029$
$^{238}\text{Pu}$	$1.094\pm 0.030$	$1.243\pm 0.031$	$1.282\pm 0.032$	$1.237\pm 0.031$	$1.077\pm 0.030$
$^{239}\text{Pu}$	$0.982\pm 0.008$	$1.011\pm 0.008$	$1.029\pm 0.008$	$1.029\pm 0.007$	$1.021\pm 0.007$
$^{240}\text{Pu}$	-	-	-	$0.993\pm 0.037$	-
$^{241}\text{Pu}$	$0.993\pm 0.022$	$0.994\pm 0.022$	$1.007\pm 0.022$	$1.011\pm 0.022$	$0.995\pm 0.022$

uncertainties. Results obtained for  $^{235}\text{U}$  were already discussed in Ref. [6]. The PROFIL trends are in better agreement with the fission yields recommended in the US library, but our fission yields are systematically lower. This bias could be due to an unrecognized systematic source of uncertainties. As a result, the PROFIL trends can be introduced in the experimental data base used for producing evaluated fission yield libraries by keeping in

TABLE III: Comparison of the effective cumulative fission yields obtained in this work with the cumulative fission yields reported in the JEFF-3.1.1 and ENDF/B-VII.1 libraries at 400 keV and 500 keV, respectively.

fissile isotope	Neodymium isotope	JEFF-3.1.1 (a)	ENDF/B-VII.1 (b)	This work (c)	Ratio (a)/(c)	Ratio (b)/(c)
$^{235}\text{U}$	$^{143}\text{Nd}$	0.05533 (1.0%)	0.05731 (0.5%)	0.05605 (2.1%)	0.987	1.022
	$^{145}\text{Nd}$	0.03796 (1.8%)	0.03776 (0.5%)	0.03703 (2.2%)	1.025	1.020
	$^{146}\text{Nd}$	0.02927 (1.8%)	0.02921 (0.5%)	0.02826 (2.4%)	1.036	1.034
	$^{148}\text{Nd}$	0.01697 (1.2%)	0.01683 (0.5%)	0.01636 (2.4%)	1.037	1.029
	$^{150}\text{Nd}$	0.00702 (2.4%)	0.00686 (0.5%)	0.00660 (2.4%)	1.063	1.039
$^{238}\text{U}$	$^{143}\text{Nd}$	0.04680 (2.4%)	0.04622 (0.7%)	0.04824 (3.5%)	0.970	0.958
	$^{145}\text{Nd}$	0.03883 (5.3%)	0.03809 (0.7%)	0.04059 (3.6%)	0.957	0.938
	$^{146}\text{Nd}$	0.03573 (5.1%)	0.03446 (0.7%)	0.03672 (3.8%)	0.973	0.938
	$^{148}\text{Nd}$	0.02296 (1.6%)	0.02112 (0.7%)	0.02249 (3.8%)	1.021	0.939
	$^{150}\text{Nd}$	0.01311 (3.7%)	0.01273 (1.0%)	0.01371 (3.8%)	0.956	0.929
$^{238}\text{Pu}$	$^{143}\text{Nd}$	0.04517 (30.5%)	0.04535 (16.0%)	0.04122 (3.7%)	1.096	1.100
	$^{145}\text{Nd}$	0.03394 (31.9%)	0.03236 (16.0%)	0.02717 (4.0%)	1.249	1.191
	$^{146}\text{Nd}$	0.02782 (32.5%)	0.02767 (16.0%)	0.02157 (4.2%)	1.290	1.277
	$^{148}\text{Nd}$	0.01689 (34.3%)	0.01757 (23.0%)	0.01359 (4.1%)	1.243	1.283
	$^{150}\text{Nd}$	0.00860 (37.5%)	0.00978 (32.0%)	0.00797 (4.0%)	1.079	1.227
$^{239}\text{Pu}$	$^{143}\text{Nd}$	0.04296 (1.3%)	0.04328 (0.4%)	0.04374 (2.3%)	0.982	0.989
	$^{145}\text{Nd}$	0.03037 (2.2%)	0.02999 (0.5%)	0.03004 (2.4%)	1.011	0.998
	$^{146}\text{Nd}$	0.02527 (2.1%)	0.02455 (0.5%)	0.02455 (2.6%)	1.029	1.000
	$^{148}\text{Nd}$	0.01696 (1.7%)	0.01658 (0.4%)	0.01647 (2.5%)	1.030	1.007
	$^{150}\text{Nd}$	0.01005 (1.9%)	0.00993 (0.5%)	0.00984 (2.6%)	1.021	1.009
$^{240}\text{Pu}$	$^{148}\text{Nd}$	0.01798 (5.0%)	0.01774 (2.0%)	0.01812 (4.4%)	0.992	0.979
$^{241}\text{Pu}$	$^{143}\text{Nd}$	0.04593 (2.6%)	0.04671 (1.0%)	0.04627 (3.1%)	0.993	1.010
	$^{145}\text{Nd}$	0.03272 (2.6%)	0.03327 (1.0%)	0.03291 (3.2%)	0.994	1.011
	$^{146}\text{Nd}$	0.02740 (2.6%)	0.02806 (1.0%)	0.02721 (3.3%)	1.007	1.031
	$^{148}\text{Nd}$	0.01945 (2.5%)	0.01956 (1.0%)	0.01922 (3.3%)	1.012	1.018
	$^{150}\text{Nd}$	0.01199 (2.7%)	0.01230 (1.0%)	0.01205 (3.3%)	0.995	1.021

mind such a systematic bias. For  $^{238}\text{Pu}$ , fast cumulative fission yields are poorly known and the present results could significantly improve the content of these libraries.

### C. Systematic variation with the mass number

The systematic variation of the fast cumulative fission yields as a function of Neodymium mass number are presented in Fig. 4. The results are normalized to  $\bar{Y}_c(^{148}\text{Nd})$ . Two isotopic chains with  $Z_{CN} = 92$  and  $Z_{CN} = 94$  are compared, corresponding to an isotonic series ranging from  $N_{CN} = 144$  to  $N_{CN} = 148$ . For Plutonium isotopes, the observed variations follow "parabolic" trends, indicated by "eye-guide" curves. As expected for heavy fission-fragments, the mass yields for the studied fissioning systems decrease with different slopes. The higher  $N_{CN}$  is, the weaker is the variation with the Nd mass number. Cumulative fission yields for  $^{235}\text{U}$  follow a similar trend, while those for  $^{238}\text{U}$  have different behaviors

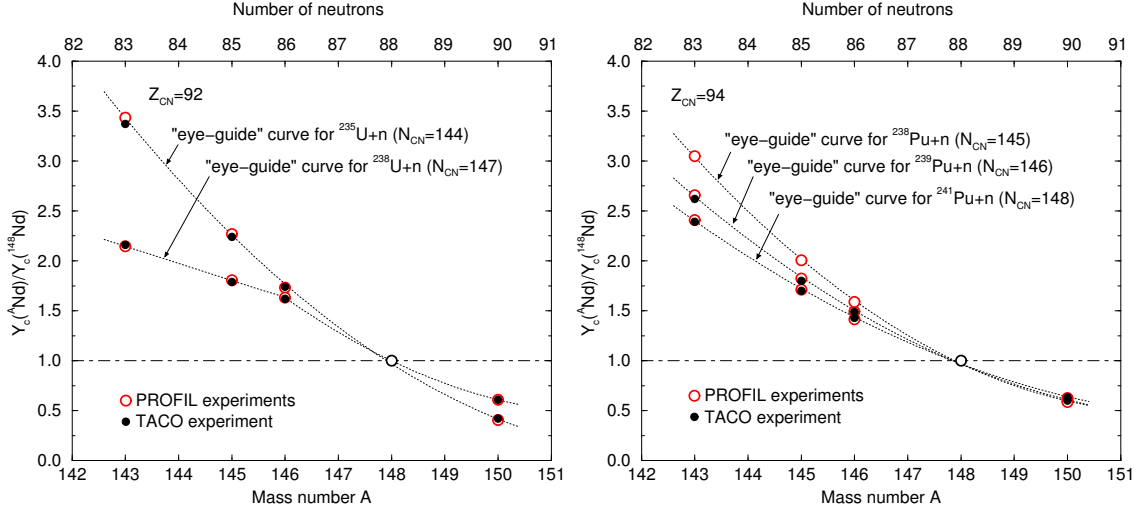


FIG. 4: Fast cumulative fission yields as a function of Nd mass number deduced from the PROFIL experiments for Uranium (left-hand plot) and Plutonium (right-hand plot) isotopes normalized to  $\bar{Y}_c(^{148}\text{Nd})$ . Our results are compared with those obtained from the interpretation of the TACO experiment [17, 18].

from either side of  $A=146$ .

In view of confirming the trend for  $^{238}\text{U}$ , we have compared the PROFIL results with cumulative fission yields extracted from the TACO experiment [17, 18]. Both experiments are based on the same principle. In the case of the TACO experiment, samples of separated isotopes were irradiated in the fast reactor RAPSODIE (CEA Cadarache, France). Even if the neutron spectrum in PROFIL is slightly softer than the TACO spectrum, results provided by the two experiments are in excellent agreement and confirm the singular variation observed for  $^{238}\text{U}$ .

As complementary results, the PROFIL trend for  $^{235}\text{U}$  and  $^{238}\text{U}$  is compared in Fig. 5 with effective cumulative fission yields  $\bar{Y}_{c_G}(^A\text{Nd})$  calculated with Eq. (5) by using results of the GEF code. The semi-empirical model implemented in GEF is able to follow the general trend of the experimental cumulative fission yields for  $^{235}\text{U}$ . The theoretical calculations suggest a smooth variation with the Nd mass number which is confirmed by the PROFIL results. For  $^{238}\text{U}$ , the behavior with the Nd mass number is not as smooth as for  $^{235}\text{U}$ . The deviation of GEF from the experimental result is somewhat amplified due to the normalization of the yields at  $A = 148$ . On an absolute scale, the value for  $^{143}\text{Nd}$  does not deviate so much, and

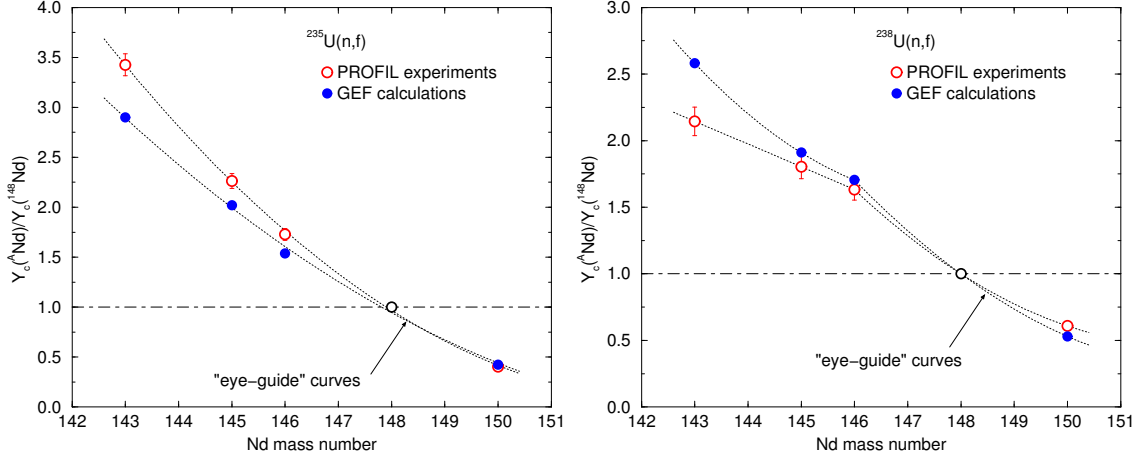


FIG. 5: Comparison of the fast cumulative fission yields deduced from the PROFIL experiments and calculated with the GEF code for  $^{235}\text{U}(n,f)$  and  $^{238}\text{U}(n,f)$ . Results are given as a function of the Nd mass number and normalized at  $A = 148$ .

GEF results seem to become too low towards the heavier Nd isotopes. Since cumulative fission yields results from a complex summation of all contributions over the entire decay time after a fission event, the origin of such a deviation from the experimental trend is therefore difficult to identify. It could reflect a general smooth trend of the GEF code, rather than a more complex structural problem such as shell closure effects that govern the odd-even staggering in the heavy fission-fragment peak. More work is probably needed for improving the description of the "super-asymmetric fission channel" introduced in the GEF code. In that case, the success of the model strongly depends on the accuracy of the experimental fission-fragment yield distributions. Promising results with an unprecedented mass resolution were already obtained in the frame of the SOFIA experiment, but for  $^{238}\text{U}$  electromagnetic fission which could be related to fission of  $^{237}\text{U}$  induced by neutrons of 8-9 MeV incident energies. A detailed discussion that allows to understand the difficulty of interpreting our results can be found in Ref. [19].

## IV. CUMULATIVE FISSION YIELDS IN THE THERMAL ENERGY RANGE

### A. Methodology

The originality of the present work consists in estimating cumulative fission yields at the thermal energy ( $E_{th} = 25.3$  meV) by combining experimental results provided by the PROFIL experiments with theoretical calculations from the GEF code. The problem can be reduced to Eq. (6). For solving this equation, we can use standard Integral Data Assimilation (IDA) procedures [8]. In that case, the unknown free parameters are the energy dependent cumulative fission yields  $Y_{cG}^X(^A\text{Nd}, E)$ . They have to be adjusted with a least-square method on the PROFIL data to satisfy Eq. (6). The IDA procedure requires prior information on the variances and covariances between the free parameters. The weakness of the IDA procedure is often the dependence of the posterior results to the prior covariance matrix. The alternative solution consists in determining the normalization factor  $N$  of Eq. (5) by considering the GEF results as shape data. This second approach is valid if the thermal and fast cumulative fission yields are strongly correlated.

The two approaches were used to determine the thermal cumulative fission yields of the Neodymium isotopes for  $^{235}\text{U}$ . Prior covariance matrix was generated by randomly varying model parameters of the GEF code [20]. The obtained covariance matrix was then modified by adding defect model contributions calculated as the difference between the evaluated values from JEFF-3.1.1 and the GEF calculations at 23.5 meV, 400 keV and 14 MeV. Prior relative uncertainties and correlation matrix for  $Y_{cG}^{235\text{U}}(^{148}\text{Nd}, E)$  are shown in the left-hand plot of Fig. 6. In the energy range of interest for this work, large relative uncertainties of about 14% are reached and correlation coefficients are close to unity. The least-square model of the CONRAD code [21] was used to produce the posterior results presented in the right-hand plot of Fig. 6. The integral assimilation of the PROFIL data lead to a significant decrease of the relative uncertainties over a wide energy range. Below 1 MeV, the final uncertainty ( $< 3\%$ ) is consistent with the uncertainties reported in column (c) of Table III. One of the remarkable results is also emphasized in Fig. 7. The arrows at 23.5 meV, 400 keV and 14 MeV show the good agreement of our posterior CONRAD calculations with the cumulative fission yields of JEFF-3.1.1. This agreement is confirmed by the detailed comparison given in the same figure between the evaluated values and results

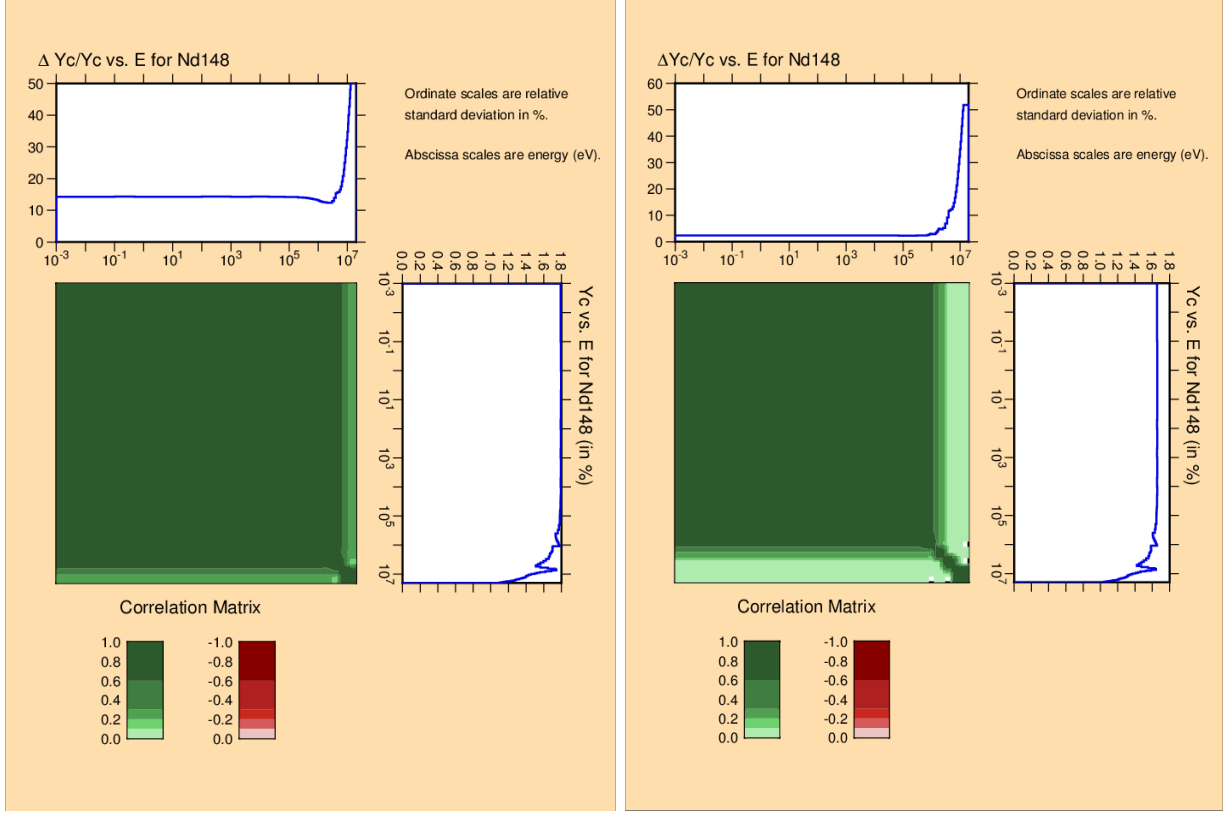


FIG. 6: Cumulative fission yields of  $^{148}\text{Nd}$  for  $^{235}\text{U}$  calculated with the GEF code as a function of the incident neutron energy, together with the relative uncertainties and correlation matrix, before (left-hand plot) and after (right-hand plot) integral assimilation of the PROFIL data. Uncertainty propagation calculations were performed with the CONRAD code [21]. The two plots were generated with the NJOY code [22].

deduced from each PROFIL experiment. At the thermal energy, the cumulative fission yield of  $^{148}\text{Nd}$  provided by the IDA procedure is:

$$Y_{c_{\text{IDA}}}^{235\text{U}}(^{148}\text{Nd}, E_{th}) = 0.01656 \pm 0.00040 \text{ (2.4\%)}.$$

For comparison, the normalization of the GEF curve with the PROFIL data provides an equivalent result:

$$Y_{c_{\text{norm}}}^{235\text{U}}(^{148}\text{Nd}, E_{th}) = 0.01657 \pm 0.00041 \text{ (2.5\%)}.$$

The excellent agreement between the two approaches and JEFF-3.1.1 on  $^{148}\text{Nd}$  is an

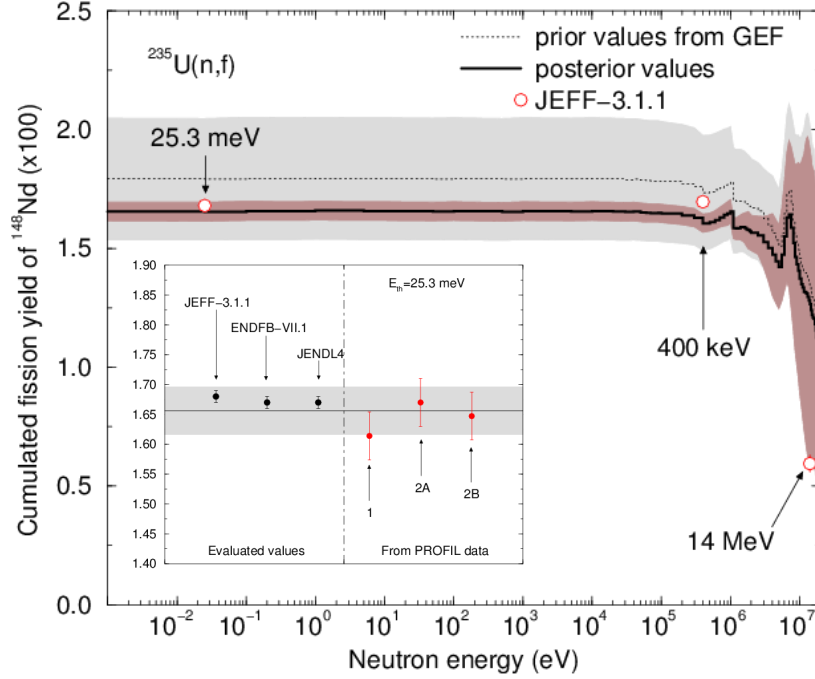


FIG. 7: Comparison of the values and uncertainties of  $Y_c^{235\text{U}}(^{148}\text{Nd}, E)$  before (prior values from GEF) and after (posterior values) integral assimilation of the PROFIL data with the CONRAD code [21]. The open circles represent the evaluated values given in the JEFF-3.1.1 fission yield library at 25.3 meV, 400 keV and 14 MeV. The inserted plot compares the cumulative fission yields of  $^{148}\text{Nd}$  for  $^{235}\text{U}$  reported in the international libraries at  $E_{th} = 25.3$  meV with the results deduced from each PROFIL experiment.

encouraging result for applying the normalization strategy instead of the more complex IDA procedure over all the PROFIL data. Table IV summarizes the cumulative fission yields obtained for  $^{235}\text{U}$  at the thermal energy. The main difference between the two methods occurs for  $^{143}\text{Nd}$ . The central values are nearly the same, but the relative uncertainty of  $\pm 11.1\%$  obtained with the IDA procedure remains too close to the prior uncertainty of  $\pm 12\%$ . Such a difference illustrates the non-negligible effect of the prior covariance matrix on the posterior uncertainty. We have to keep in mind this constraint in the interpretation of the results provided in the following sections.



TABLE IV: Cumulative fission yields of the Neodymium isotopes for  $^{235}\text{U}(n_{th},f)$  obtained at  $E_{th} = 25.3$  meV from the integral assimilation of the PROFIL data and from the normalization of the GEF results with the PROFIL data.

Neodymium isotope	prior value	Integral Data Assimilation (a)	Normalization GEF results (b)	ratio (a)/(b)
$^{143}\text{Nd}$	0.05246 (12.0%)	0.05598 (11.1%)	0.05742 (2.1%)	0.975
$^{145}\text{Nd}$	0.03678 ( 2.3%)	0.03797 ( 2.3%)	0.03814 (2.3%)	0.996
$^{146}\text{Nd}$	0.02783 ( 9.6%)	0.02881 ( 2.5%)	0.02898 (2.5%)	0.994
$^{148}\text{Nd}$	0.01792 (14.3%)	0.01656 ( 2.4%)	0.01657 (2.5%)	0.999
$^{150}\text{Nd}$	0.00746 (22.8%)	0.00657 ( 3.5%)	0.00661 (3.2%)	0.994

### B. Systematic variation with the mass number

The thermal cumulative fission yields of the Neodymium isotopes obtained after normalization of the GEF calculations with the PROFIL data are reported in Table V. The comparison with the evaluated data, reported in JEFF-3.1.1 and ENDF/B-VII.1, confirms that our methodology can provide reliable thermal values for  $^{235}\text{U}$ ,  $^{239}\text{Pu}$  and  $^{241}\text{Pu}$ . As already observed in the fast energy range, the agreement remains within the limit of the reported uncertainties. In the case of the  $^{235}\text{U}(n,f)$  reaction, our result for  $^{148}\text{Nd}$  is 1.4% and 1% lower than the one recommended in JEFF-3.1.1 and ENDFB/-VII.1 libraries, respectively. These differences lie below the PROFIL uncertainty. The present work also provides valuable tendencies on the poorly known cumulative fission yields for the  $^{238}\text{Pu}(n_{th},f)$  and  $^{240}\text{Pu}(n_{th},f)$  reactions. For  $^{238}\text{Pu}$ , the good agreement obtained between our results and JEFF-3.1.1 at  $A = 143$  and  $A = 145$  contributes to support the combine analysis of the PROFIL results with the GEF calculations. Cumulative fission yields at thermal energy for  $^{238}\text{U}$  are only given for comparison. The present approach are probably not adequate in that case. As discussed in section III C, improved GEF calculations are needed for correctly described the fast cumulative fission yields for  $^{238}\text{U}$  before extrapolating the theory in the thermal energy range.

Results reported in Table V are presented in Fig. 8 as a function of the Nd mass number. The observed behavior is nearly similar to the one shown in Fig. 4. The "eye-guide" curves

TABLE V: Comparison of the thermal cumulative fission yields obtained in this work with those reported at 23.5 meV in the JEFF-3.1.1 and ENDF/B-VII.1 libraries.

fissile isotope	Neodymium isotope	JEFF-3.1.1 (a)	ENDF/B-VII.1 (b)	This work (c)	Ratio (a)/(c)	Ratio (b)/(c)
$^{235}\text{U}$	$^{143}\text{Nd}$	0.05954 (1.4%)	0.05956 (0.4%)	0.05742 (2.1%)	1.037	1.037
	$^{145}\text{Nd}$	0.03955 (1.1%)	0.03933 (0.4%)	0.03814 (2.3%)	1.037	1.031
	$^{146}\text{Nd}$	0.02987 (1.0%)	0.02997 (0.4%)	0.02898 (2.5%)	1.031	1.034
	$^{148}\text{Nd}$	0.01681 (0.7%)	0.01674 (0.4%)	0.01657 (2.5%)	1.014	1.010
	$^{150}\text{Nd}$	0.00651 (1.0%)	0.00653 (0.5%)	0.00661 (3.2%)	0.985	0.989
$^{238}\text{U}$	$^{143}\text{Nd}$			0.05580 (3.5%)		
	$^{145}\text{Nd}$			0.05112 (3.6%)		
	$^{148}\text{Nd}$			0.02949 (3.8%)		
	$^{150}\text{Nd}$			0.01637 (3.9%)		
$^{238}\text{Pu}$	$^{143}\text{Nd}$	0.03911 ( 5.7%)		0.04119 (4.0%)	0.950	
	$^{145}\text{Nd}$	0.02704 ( 6.0%)		0.02714 (4.2%)	0.996	
	$^{146}\text{Nd}$	0.01277		0.02155 (4.4%)	0.593	
	$^{148}\text{Nd}$	0.00863		0.01359 (4.3%)	0.635	
	$^{150}\text{Nd}$	0.00586 (71.2%)		0.00797 (4.4%)	0.735	
$^{239}\text{Pu}$	$^{143}\text{Nd}$	0.04476 (1.1%)	0.04413 (0.5%)	0.04502 (2.3%)	0.994	0.980
	$^{145}\text{Nd}$	0.03036 (1.1%)	0.02982 (0.4%)	0.03062 (2.4%)	0.992	0.974
	$^{146}\text{Nd}$	0.02496 (1.0%)	0.02458 (0.4%)	0.02501 (2.6%)	0.998	0.983
	$^{148}\text{Nd}$	0.01658 (1.0%)	0.01642 (0.5%)	0.01683 (2.6%)	0.985	0.976
	$^{150}\text{Nd}$	0.00975 (1.3%)	0.00966 (0.4%)	0.00981 (2.8%)	0.994	0.985
$^{240}\text{Pu}$	$^{148}\text{Nd}$		0.01772 (23.0%)	0.01860 (4.5%)		0.953
$^{241}\text{Pu}$	$^{143}\text{Nd}$	0.04380 (2.1%)	0.04578 (0.7%)	0.04681 (3.1%)	0.935	0.978
	$^{145}\text{Nd}$	0.03141 (2.9%)	0.03263 (1.0%)	0.03337 (3.2%)	0.941	0.978
	$^{146}\text{Nd}$	0.02657 (2.6%)	0.02766 (0.7%)	0.02751 (3.3%)	0.966	1.005
	$^{148}\text{Nd}$	0.01881 (3.4%)	0.01932 (0.7%)	0.01927 (3.3%)	0.976	1.002
	$^{150}\text{Nd}$	0.01154 (2.8%)	0.01209 (1.0%)	0.01195 (3.4%)	0.966	1.012

follow a "parabolic" shape, which is consistent with the behavior of the cumulative fission yields evaluated in JEFF-3.1.1. It is also correctly predicted by the GEF calculations. For the  $^{235}\text{U}(n,f)$  reaction, results obtained with the IDA and normalization procedures (Table IV) are reported in the same plot. Both procedures provide a similar trend. The singular behavior for  $^{238}\text{U}$  is still visible. However, the abrupt variation with the Nd mass number is more pronounced than in the fast energy range and the differences with GEF (prior values) are rather large. As a result, our thermal cumulative fission yields for the  $^{238}\text{U}(n_{th},f)$  reaction should be taken with care.

### C. Systematic variation from thermal to fast energy ranges

Detailed discussions on the variation of cumulative fission yields with the incident neutron energy are scarce in the literature and the specific behavior of the Neodymium isotopes is not well documented. As indicated by Britt [23], it exists in the literature some experimental evidences of the weak energy-dependence of fission yields in the immediate vicinity of the

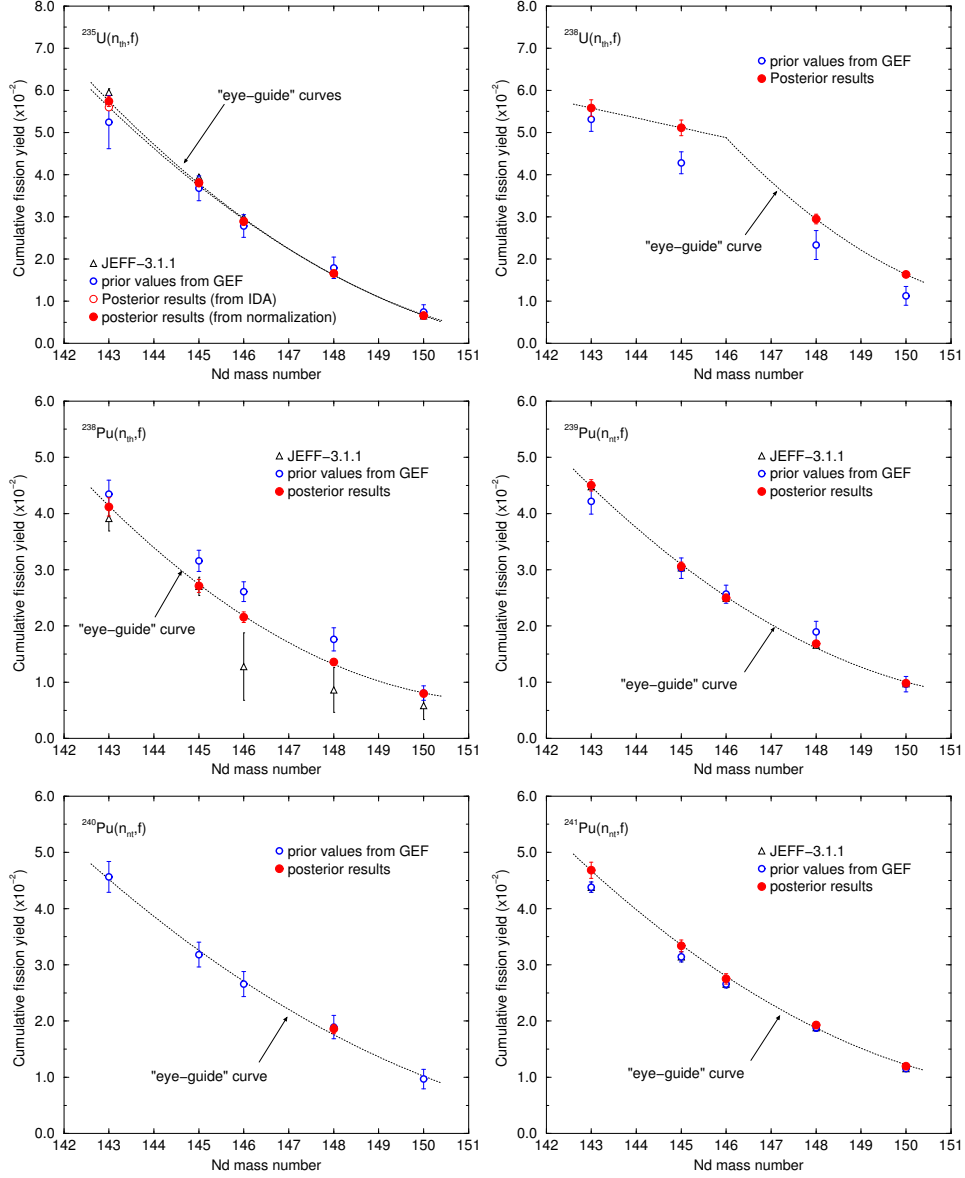


FIG. 8: Variation of the thermal cumulative fission yields with the Nd mass number. The posterior results were obtained after normalization of the GEF trends with the PROFIL data. They are compared with the prior GEF calculations and the evaluated values reported in JEFF-3.1.1. For  $^{235}\text{U}$ , the thermal cumulative fission yields obtained from the integral assimilation of the PROFIL data is also shown.

heavy mass peak. The issue for the  $^{235}\text{U}(n,f)$  and  $^{239}\text{Pu}(n,f)$  reactions from the thermal to fast energy ranges was qualitatively addressed by Maeck [24, 25] in the beginning of the 80s by using the cumulative ratio  $^{150}\text{Nd}/^{148}\text{Nd}$  as an energy index. More recently, two

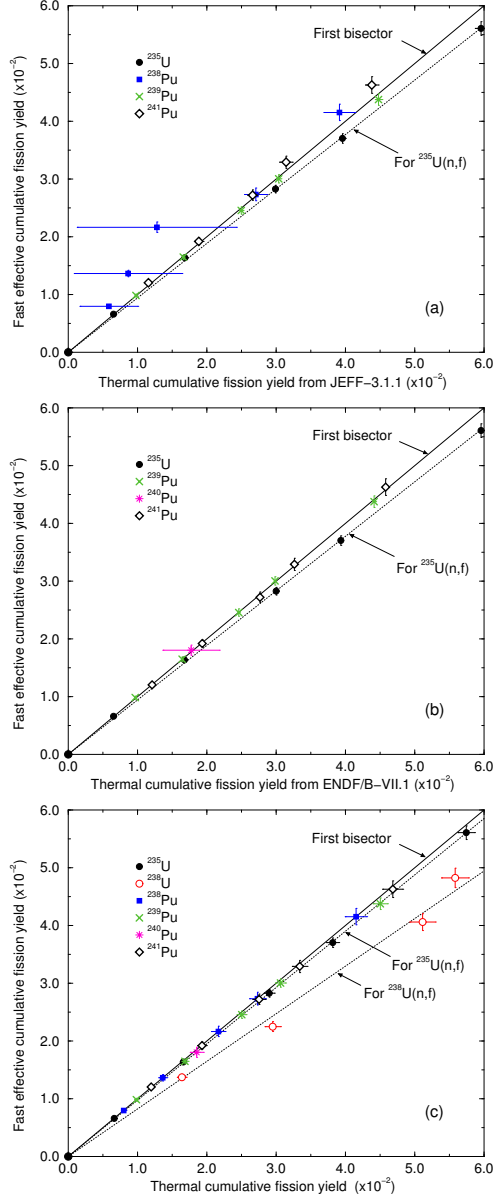


FIG. 9: Effective cumulative fission yields of the Neodymium isotopes determined with the PROFIL trends in the fast energy range (column (c) of Table III) as a function of the thermal values reported in columns (a), (b) and (c) of Table V. The solid line represents the first bisector. The dotted lines are "eye-guide" lines that follow the trends obtained for  $^{235}\text{U}(n,f)$  and  $^{238}\text{U}(n,f)$ .

integral experiments in mostly thermal and epithermal neutron spectra have confirmed the fluctuations of the  $^{235}\text{U}$  cumulative fission yields in the resonance range of the neutron cross sections [26]. However, for the Nd mass number, a variation lower than 1% is expected. As a result, since rather low relative uncertainties of about 1% are difficult to achieve, variations

observed in the evaluated fission yield libraries between the thermal and fast energies could mainly reflect the accuracy and the dispersion of the experimental values introduced in the evaluation procedure. One of the recurrent problems is also the definition of the "fast energies". In JEFF-3.1.1, it is set to  $E_n = 400$  keV, while  $E_n = 500$  keV has been chosen in ENDF/B-VII.1. This difference of 100 keV is difficult to explain and probably not justified for fast cumulative fission yields. Indeed, data introduced in the evaluation procedure are usually measured in fast neutron spectra of different hardness, for which the mean excitation energy of fissioning events is scarcely reported in the literature. In the present work, our results are not affected by these considerations because we directly provide effective values valid for typical sodium fast reactors (SFR).

The variation of the cumulative yields of the Neodymium isotopes with the neutron energy is illustrated in Fig. 9. We decided to display the effective values determined with the PROFIL trends in the fast energy range (column (c) of Table III) as a function of the thermal values. Abscissa of top and middle plots represents the thermal values evaluated in the JEFF-3.1.1 and ENDF/B-VII.1 libraries (column (a) and (b) of Table V). Abscissa of bottom plot is related to results obtained from the normalization of the GEF calculations with the PROFIL trends (column (c) of Table V). The dispersion of the results around the first bisector provides valuable information on the correlation between the thermal and fast energy ranges as a function of the fission yields.

For  $^{235}\text{U}(n,f)$ , we can observe a systematic deviation from the first bisector which increases with the fission yields value. In the bottom plot, the deviation is in the limit of our experimental uncertainties. This trend could be a mathematical artefact coming from the normalization strategy applied to the GEF results. As indicated in Table IV, the difference with the IDA procedure is maximal for the cumulative fission yield of  $^{143}\text{Nd}$  and reaches 2.5%. For  $^{239}\text{Pu}(n,f)$ , a weak energy dependence regardless of the fission yield value is suggested by all the three plots. A similar conclusion arises from our results for  $^{241}\text{Pu}(n,f)$ . This trend is fully confirmed by the US library, but in contradiction with JEFF-3.1.1. This raises problems related to the reliability of the theoretical calculations and of the normalization strategy. Since we have used the GEF data as shape data, the behavior between the fast and thermal energy ranges are fully correlated and depend on the semi-empirical model implemented in GEF. The satisfactory agreement with the evaluated cumulative fission yields of the Neodymium isotopes for  $^{235}\text{U}$ ,  $^{239}\text{Pu}$  and  $^{241}\text{Pu}$  (ratio (a)/(c) and (b)/(c))

in Table V) could be seen as a probe of the capabilities of GEF to correctly predict the weak energy-dependence up to neutron energies of interest for SFR.

Once more, questions emerge from the singular behavior of the cumulative fission yields for  $^{238}\text{U}(\text{n},\text{f})$ . Further advanced theoretical investigations are needed, such as those conducted in Refs [27–29]. Models which calculate the mass distribution theoretically, and do not rely on a fit to experimental data, should provide informative systematics for a series of systems along isotopic chains as a function of the compound-nucleus excitation energy.

## V. CONCLUSIONS

The present work demonstrates the possibility of combining theoretical calculations from the GEF code with integral trends measured in a fast neutron spectrum to determine thermal values consistent with those evaluated in international nuclear data libraries. The accuracy of the obtained cumulative fission yields ranges from 2% to 5%. Such rather low relative uncertainties are mainly driven by the accurate calculated-to-experimental ratios deduced from the PROFIL experiments.

The cumulative fission yields of the Neodymium isotopes for neutron-induced fission of  $^{235}\text{U}$ ,  $^{238}\text{Pu}$ ,  $^{239}\text{Pu}$ ,  $^{240}\text{Pu}$  and  $^{241}\text{Pu}$  exhibit a smooth variation as a function of the Nd mass number and a weak energy-dependence from thermal to fast energy ranges. For the isotopic chain  $Z_{CN} = 94$ , the energy-dependence is even negligible in the case of sodium fast reactor applications.

For the  $^{238}\text{U}(\text{n},\text{f})$  reaction, the behavior of the Nd cumulative fission yields is more complex and needs deeper theoretical works to be correctly understood. Improved modelisation of the fission process depends on the accuracy of the experimental yield distributions. Recent data obtained in the frame of the SOFIA experiment with an unprecedented mass resolution are promising results for solving the deviation observed between our PROFIL results and GEF calculations.

## Acknowledgment

The authors would like to thanks Virginie Huy, from CEA of Cadarache, for her contribution in the interpretation of the spectral indices measured in the FCA facilities.

- 
- [1] J.M. Ruggieri *et al*, ERANOS 2.1: the international code system for GEN-IV fast reactor analysis, *Proc. Int. Congress on Advances in Nuclear Power Plants, ICAPP06*, Reno, USA, 2006.
- [2] J. Tommasi *et al*, Analysis of Sample Irradiation Experiments in PHENIX for JEFF-3.0 Nuclear Data Validation, *Nucl. Sci. Eng.*, **154**, 119 (2006).
- [3] J. Tommasi *et al*, Analysis of the PROFIL and PROFIL-2 Sample Irradiation Experiments in PHENIX for JEFF-3.1 Nuclear Data Validation, *Nucl. Sci. Eng.*, **160**, 232 (2008).
- [4] E. Privas *et al*, The use of nuclear data as nuisance parameters in the integral data assimilation of the PROFIL experiments, *Nucl. Sci. Eng.*, **182**, 377 (2016).
- [5] N. Terranova, Covariance evaluation for nuclear data of interest to the reactivity loss estimation of the Jules Horowitz material testing reactor, PhD Thesis, Aix-Marseille University, France, 2016.
- [6] E. Privas *et al*, Measurements of the effective cumulative fission yields of  $^{143}\text{Nd}$ ,  $^{145}\text{Nd}$ ,  $^{146}\text{Nd}$ ,  $^{148}\text{Nd}$  and  $^{150}\text{Nd}$  for  $^{235}\text{U}$  in the PHENIX fast reactor, *EPJ Nuclear Sci. Technol.*, **2**, 32 (2016).
- [7] K.-H. Schmidt *et al*, General Description of Fission Observables: GEF Model Code, *Nucl. Data Sheets*, **131**, 107 (2016).
- [8] C. De Saint Jean *et al*, to be published in *Nucl. Data Sheets*.
- [9] A. Santamarina *et al*, The JEFF-3.1.1 Nuclear Data Library, Nuclear Energy Agency, JEFF report 22, 2009.
- [10] M. B. Chadwick *et al*, ENDF/B-VII.1 nuclear data for science and technology: Cross sections, covariances, fission product yields and decay data, *Nucl. Data Sheets*, **112**, 2887 (2011).
- [11] R.W. Mills, Fission product yield evaluation, PhD Thesis, University of Birmingham, United Kingdom, 1995.
- [12] J.M. Ruggieri *et al*, JEFF-3.1 nuclear data validation for fast reactor physics, *Proc. Int. Conf. on Physics and Technology of Reactors and Applications, PHYTRA*, Marakech, Morocco, 2007.
- [13] G. Perret *et al*, Reanalysis of the Gas-cooled fast reactor experiments at the zero power facility Proteus - Spectral indices, *EPJ Web of Conferences*, **42**, 05002 (2013).



- [14] G. Perret *et al*, Toward Reanalysis of the Tight-Pitch HCLWR-PROTEUS Phase II Experiments, *EPJ Web of Conferences*, **111**, 11006 (2016).
- [15] G. Chiba *et al*, Integral test of JENDL-3.3 for Fast Reactors, *Proc. JAERI Conf.*, JAERI-Conf 2003-006, 22, 2003.
- [16] G. Rimpault, Preliminary results on FCA-IX fission chambers analysis, Expert Group on Integral Experiments for Minor Actinide Management, EGIEMAM-II, 2016.
- [17] M. Robin *et al*, The importance of fission product nuclear data in burnup determination, *Proc. Int. Conf. on Chemical and Nuclear Data*, Canterbury, UK, 1973.
- [18] L. Koch, Systematics of fast cumulative fission yields, *Radio. Acta* **29**, 61 (1981).
- [19] E. Pellereau *et al*, Accurate isotopic fission yields of electromagnetic-induced fission of  $^{238}\text{U}$  in inverse kinematics at relativistic energies, *Phys. Rev. C*, **95**, 054603(2017).
- [20] O. Leray *et al*, "Fission yield covariances for JEFF: A Bayesian Monte Carlo method, *EPJ Web of Conferences*, **146**, 09023 (2017).
- [21] P. Archier *et al*, CONRAD evaluation code: development status and perspectives, *Nucl. Data Sheets*, **118**, 488 (2014).
- [22] R.E. MacFarlane and A.C. Kahler, Methods for Processing ENDF/B-VII with NJOY, *Nucl. Data Sheets*, **111**, 2739 (2010).
- [23] H.C. Britt *et al*, Review of the status of cumulative fission yields from  $^{239}\text{Pu}(n,f)$  of interest to nuclear forensics, Lawrence Livermore National Laboratory, Report LLNL-TR-459777, 2010.
- [24] W.J. Maeck, The correlation of  $^{235}\text{U}$  thermal and fast reactor fission yields with neutron energy, Exxon Nuclear Idaho Company, Inc. Report ENICO-1065, 1980.
- [25] W.J. Maeck, The correlation of  $^{239}\text{Pu}$  thermal and fast reactor fission yields with neutron energy, Exxon Nuclear Idaho Company, Inc., Report ENICO-1099, 1981.
- [26] P. Leconte, J-P. Hudelot and M. Antony, Fluctuation of mass yield distribution for the epithermal fission of  $^{235}\text{U}$  and its impact on HCLWR calculations, *Nucl. Sci. Eng.* **172**, 208 (2012).
- [27] O. Litaize, O. Serot and L. Berge, *Eur. Phys. J.* **A51**, 177 (2015).
- [28] P. Moller and C. Schmitt, Evolution of uranium fission-fragment charge yields with neutron number, *Eur. Phys. J. A*, **53** (2017).
- [29] A.J. Sierk, Langevin model of low-energy fission, *Phys. Rev. C*, **96**, 034603 (2017).